ACTA UNIVERSITARIA
Multidisciplinary Scientific Journal

| VOLUMEN 29 | 2019 |
ISSN online 2007-9621
http://doi.org/10.15174/au.2019.1734

Effect of temperature, pressure and power in obtaining TiO_2 and TiO_2-Fe via microwaves and evaluation of photocatalytic activity with synthesis time

Efecto de la temperatura, presión y potencia en la obtención de TiO_2 y TiO_2-Fe vía microondas y evaluación de la actividad fotocatalítica con el tiempo de síntesis

Ulises Zurita-Luna[1], Juan Zárate-Medina[2]*, Anayeli Y. Gallegos-Hernández[3], Rafael Romero-Toledo[4], José Apolinar-Cortés[1]

[1]Facultad de Ingeniería Química, Universidad Michoacana de San Nicolás de Hidalgo.
[2]Instituto de Investigación en Metalurgia y Materiales, Ciudad Universitaria, S/N, Morelia, Michoacán, 58060, México.
[3]División de Materiales Avanzados Instituto Potosino de Investigación Científica y Tecnológica.
[4]Departamento de Ingeniería Química, División de Ciencias Naturales y Exactas, Universidad de Guanajuato.
E-mail: jzaratemedina@gmail.com
*Corresponding author.

Abstract

Photocatalysts of titanium dioxide (TiO_2) doped with different percentages of iron were synthesized via microwave at 180 °C, with two different times, 2 min and 10 min. Temperature, pressure, and power change were analyzed. Important changes were mainly observed in the pressure conditions. The synthesized photocatalysts were characterized using: scanning electron microscopy (SEM), X-ray diffraction (XRD), specific surface area (BET), and UV-vis diffuse reflectance spectroscopy. The presence of nanoparticles was observed; furthermore, anatase crystalline phase of TiO_2 was the only found. A study of the photocatalytic activity for discoloration acid blue dye 9 (AB9) with UV light was performed, and it was compared with the commercial photocatalyst Degussa P-25, being the best result a total discoloration of dye at 45 min of reaction using the TiO_2 photocatalyst undoped synthesized at 2 min. The iron doping did not show an improvement in the photocatalytic activity, and it was also observed that the time of synthesis considerably influences in the photocatalytic activity, with best efficiencies at minor synthesis time.

Keywords: Doping of TiO_2; heterogeneous photocatalysis; microwave synthesis.

Resumen

Fotocatalizadores de dióxido de titanio (TiO_2) dopados a diferentes porcentajes de hierro fueron sintetizados vía microondas a 180 °C a dos tiempos: 2 min y 10 min de síntesis, en los cuales se analizó el cambio de temperatura, presión y potencia. Se observaron variaciones importantes, principalmente en las condiciones de presión. Los fotocatalizadores sintetizados fueron caracterizados usando: microscopía electrónica de barrido, difracción de rayos X, área superficial específica y espectroscopía UV-vis de reflectancia difusa. Se observó la presencia de nanopartículas; además, la fase anatasa cristalina de TiO_2 fue la única encontrada. Se realizó un estudio de la actividad fotocatalítica para la decoloración del colorante azul ácido 9 con luz UV, la cual se comparó con el fotocatalizador comercial Degussa P-25, teniendo como mejor resultado una decoloración total del colorante a 45 min de reacción con el fotocatalizador de TiO_2 sin dopar sintetizado a 2 min de reacción. El dopaje con hierro no presentó una mejor actividad fotocatalítica; además, se observó que el tiempo de síntesis influye considerablemente en la actividad fotocatalítica, teniendo mejores eficiencias en el menor tiempo.

Palabras clave: Dopaje de TiO_2; fotocatálisis heterogénea; síntesis vía microondas.

Recibido: 2 de enero de 2017 Aceptado: 10 de enero de 2019 Publicado: 08 de abril de 2019

Como citar: Zurita-Luna. U., Zárate-Medina, J., Gallegos-Hernández, A. Y., Romero-Toledo, R., & Apolinar Cortés, J. (2019). Effect of temperature, pressure and power in obtaining TiO_2 and TiO_2-Fe via microwaves and evaluation of photocatalytic activity with synthesis time. *Acta Universitaria* 29, e1734. doi. http://doi.org/10.15174.au.2019.1734

ISSN online 2007-9621

Introduction

The use of titanium dioxide (TiO_2) in photocatalysis is very promising (López-Muñoz, Arencibia, Segura & Raez, 2017; Xiang *et al.*, 2018) and has attracted great interest for the mineralization of pollutants in both air and water (Song, You, Chen & Jia, 2015; Yu & Lee, 2007). The above is mentioned since TiO_2 has the properties of photostability and non-toxicity as well as being relatively abundant in nature and an economic compound (Shojaie & Loghmani, 2010). One drawback, up to now, is its low performance in the photocatalytic activity; however, in recent times, properties and conditions that improve photocatalytic activity have been studied. One option is the modification of the TiO_2 by incorporating transition metals and other cations, causing changes in the electronic properties (Kim, Lee, Kim, Chung & Kim, 2006; Wang, Lin & Yang, 2009; Yan, Tu, Chan & Jing, 2016). The introduction of iron (Fe) into the TiO_2 generally produces a shift of the absorption edge towards the visible edge and reduces the band gap. It also has the property of inhibiting the recombination of electron-hole pairs (Doong, Chang & Huang, 2009). Moreover, the catalytic role of Fe remains controversial, because it gives positive results in some studies (Adán, Bahamonde, Fernández-García & Martínez-Arias, 2007; Choi, Termin & Hoffmann, 1994) and negative results in others (Esquivel *et al.*, 2013). Some of the variants that have been observed to modify the photocatalytic activity of TiO_2 are the methods of synthesis, among which the most promising are those which can obtain and modify TiO_2 nanoparticles, such as hydrothermal treatment (Mali, Shinde, Betty, Bhosale, Lee & Patil, 2011), solvothermal process (Perera & Gillan, 2008), sol-gel method (Abbas, 2009), chemical vapor deposition (Alijani & Shariatinia, 2017; Gladfelter, 2011), and cathodic spraying (Yu & Shen, 2011), among others. These methods give different textural and structural characteristics to TiO_2. However, these processes have certain disadvantages because the synthesis times tend to be relatively long (in the order of hours or days) and inhomogeneous heating. A method of synthesis of microwave irradiation has been studied in recent years (Hamedani, Mahjoub, Khodadadi & Mortazavi, 2011; Ocakoglu *et al.*, 2015). It has been related to the preparation of TiO_2 nanoparticles, as this method produces a more uniformed heating and achieves shorter synthesis times; this is due to the fact that microwaves directly affect the compounds which can lead to higher heating rates and, thereby, time and energy saving (Komarneni, Rajha & Katsuki, 1999; Suzuki, Yamaguchi, Kageyama, Oaki & Imai, 2015). Despite the use of microwaves, which is apparently a viable method for the synthesis of TiO_2, there are still few references to its use on photocatalysis (Khade, Suwarnkar, Gavade & Garadkar, 2015; Tian *et al.*, 2015). The references found in the literature use synthesis times, which could be shorter, offering characteristics such as good structural, morphological, and photocatalytic activity. This is due to the time, which is an important factor in the synthesis of the material since a small change in synthesis time (less than 10 min) causes a significant change in photocatalytic activity. Esquivel *et al.* (2013) performed synthesis of TiO_2 doped with different percentages of iron via microwave, varying the temperature and synthesis time, saying that longer synthesis times produced better results in the photocatalytic activity. However, the tests were performed at different time conditions and, because of the large number of synthesized compounds, some results were compared under different conditions, besides using a complex synthesis method with times over 20 min. Considering the benefits of the use of microwaves, the synthesis time as an important factor, and the benefits that may occur due to the incorporation of iron on TiO_2, in the present work TiO_2 and TiO_2 compounds doped with different percentages of Fe were synthesized by microwave method. The syntheses were performed at two different reaction times (under the same conditions), in which the changes of temperature, pressure, and power were analyzed. In the same way, the synthesized photocatalysts were analyzed by various characterization techniques, determining their structural, morphological, and electronic properties. A study was also conducted in the photocatalytic activity to, thereby, compare the efficiency of the photocatalysts.

ISSN online 2007-9621

Experimental

Microwave assisted synthesis

The synthesis was performed in a microwave reactor (brand Anton Paar model Synthos 3000), with a power of 600 W. The process started with the mixture of reagents. For the case of undoped TiO_2, ethyl alcohol (industrial 75%), titanium butoxide (Aldrich brand Sigma 97% purity), and deionized water were used, while for the TiO_2-Fe, in addition to the above reagents, $Fe(NO_3)_3 9H_2O$ solution (brand Golden Bell analytical reagent grade ACS) was added as a precursor of the doping agent. Subsequently, each prepared mixture was introduced in the microwave reactor, where the temperature and the reaction time were set. The suspension obtained was subjected to drying in an oven (Brand Felissa) at 100 °C for 18 h. Then a grinding process was experienced to obtain powders of less than 130ASTM mesh size. Each synthetized material underwent a heat treatment at 500 °C for one hour. The synthesis was performed at 180 °C. The effect of doping with iron was assessed by varying the weight percentage of Fe at 0%, 0.05%, 0.25%, and 1%. The effect of synthesis time in the reactor was evaluated at 2 min and 10 min after the heating ramp of 10 min. The experimental design is shown in table 1, where the intersection of the percentage of iron and the reaction time gives the compound synthesized.

Table 1. Nomenclature of the synthesized compounds.

	0% Fe	0.05% Fe	0.25% Fe	1% Fe
2 minutes	B2T180	0.05%Fe2T180	0.25%Fe2T180	1%Fe2T180
10 minutes	B10T180	0.05%Fe10T180	0.25%Fe10T180	1%Fe10T180

Source: Author's own elaboration.

Characterization

The characterization of the photocatalysts was carried out through three different techniques. First, the Scanning Electron Microscopy (SEM) was performed using a JEOL JSM-7600F microscope. Secondly, the Specific Surface Area (BET) was carried out using a Quantasorb Jr. equipment; this was determined via N_2 adsorption at 77 K; subsequently, UV-vis Spectroscopy Diffuse Reflectance, using a Jaz Sensing Spectral Suite equipment, was performed in a wavelength range of 325 nm to 650 nm in absorbance units and, finally, the X-ray diffraction (XRD) technique was applied, employing a SIEMENS D5000 diffractometer, using $K\alpha$ radiation copper (1.54 Å).

Photocatalytic activity

To determine the photocatalytic activity, a reaction system was used. Such system consists of an annular tubular batch type reactor, with constant air supply, agitation, and an external heating system at 40 °C. The irradiation source was an ultraviolet light lamp (365 nm wavelength) Tecnolite F8T5BLB of 8 W, located in the center of the reactor. The air was supplied through a fine bubble diffuser immersed on the bottom of the reactor, and the stirring system consists of a magnetic stirrer, which keeps the photocatalyst suspended. The dye used for the degradation tests was acid blue 9 (AB9) dye, with an initial concentration of 20 mg L^{-1} and the concentration of photocatalyst used was 1000 mg L^{-1} (0.23 gr photocatalyst in 230 ml of dye solution). Dye concentration measurements were done with a spectrophotometer UV/Vis JENWAY 6505, measuring the absorbance in the wavelength range of 250 nm to 750 nm. Before starting the reaction, the photocatalyst-dye suspension was kept for 30 min with the lamp off; this was in order to evaluate the adsorption process. Samples were taken every 15 min

ISSN online 2007-9621

during the process of adsorption and dye degradation reaction; they were centrifuged at 10 000 rpm for 5 min in an Eppendorf minispin centrifuge to remove the material and measure its concentration.

Results and discussion

Microwave Reactor

Conditions of pressure and temperature that occurred within the reaction vial during synthesis of the photocatalysts, as well as the power supplied by the microwave equipment, are all shown in figure 1. The microwave reactor was programmed to reach a temperature of 180 ºC in 10 min. However, due to the inertia of the same equipment, there are variations in the temperature; the results description is presented according to the real values. Figures 1b and 1d show the synthesis conditions of the compounds synthesized to 10 min reaction, 1%Fe10T180 and B10T180, respectively. It was observed in both subsections that at the beginning of the experimental, the temperature was found in the order of 22 °C and then increased until 180 °C. It is noted that although the start time of nominal reaction was set at 10 min so that it reacts at 180 °C. In the synthesis of both compounds real differences are presented. It is the order of 2 min less for the synthesis of compound B10T180 and one minute less for compound 1%Fe10T180. With respect to pressure, it increases as the temperature increases within the vial, reaching its peak at the end of the reaction, being 26.6 bars for the sample without iron B10T180 and 28.5 bars for the sample with iron 1%Fe10T180. This is also attributed to the greater absorption of energy gained by effect of the iron salt. Another possibility for the higher temperature observed with higher iron loadings could be due to decomposition of the nitrate counterions: nitrogen oxides are expected to be released upon heating and incorporation of the Fe^{3+} ions into the TiO_2 structure. Regarding power, it is observed that the power used for the synthesis of the compound with iron (1%Fe10T180) was lower than the one used for the synthesis of no iron compound (B10T180). The above mentioned was because the iron salt increased the polarity of the solution, giving greater efficiency in energy absorption. For samples synthesized at nominal 2 min of reaction (figure 1a and 1c), the ironless B2T180 compound (figure 1c) does not cause reaction because the temperature of 180 °C was reached at the end of the 2 min. In the case of the compound with iron 1%Fe2T180 (figure 1a), it was observed that it reached a temperature of 180 °C at 30 s after the programmed time. However, during the following 40 s, there was an increase of 5 °C due to the reactor controller, which caused the 180 °C; the set temperature could not remain constant at any time either. In the compounds synthesized at 10 min, the increase observed in the heating ramp of the sample 1%Fe2T180 was possibly due to the ionic salt ($Fe(NO_3)_3.9H_2O$). According to the pressure, the maximum values were 20.4 bars for sample B2T180 and 20.8 bars for 1%Fe2T180, being higher for the compound with iron. With respect to the power, a similar behavior to the compounds synthesized at 10 min reaction was observed. Lower power was supplied to the iron doped compounds.

ISSN online 2007-9621

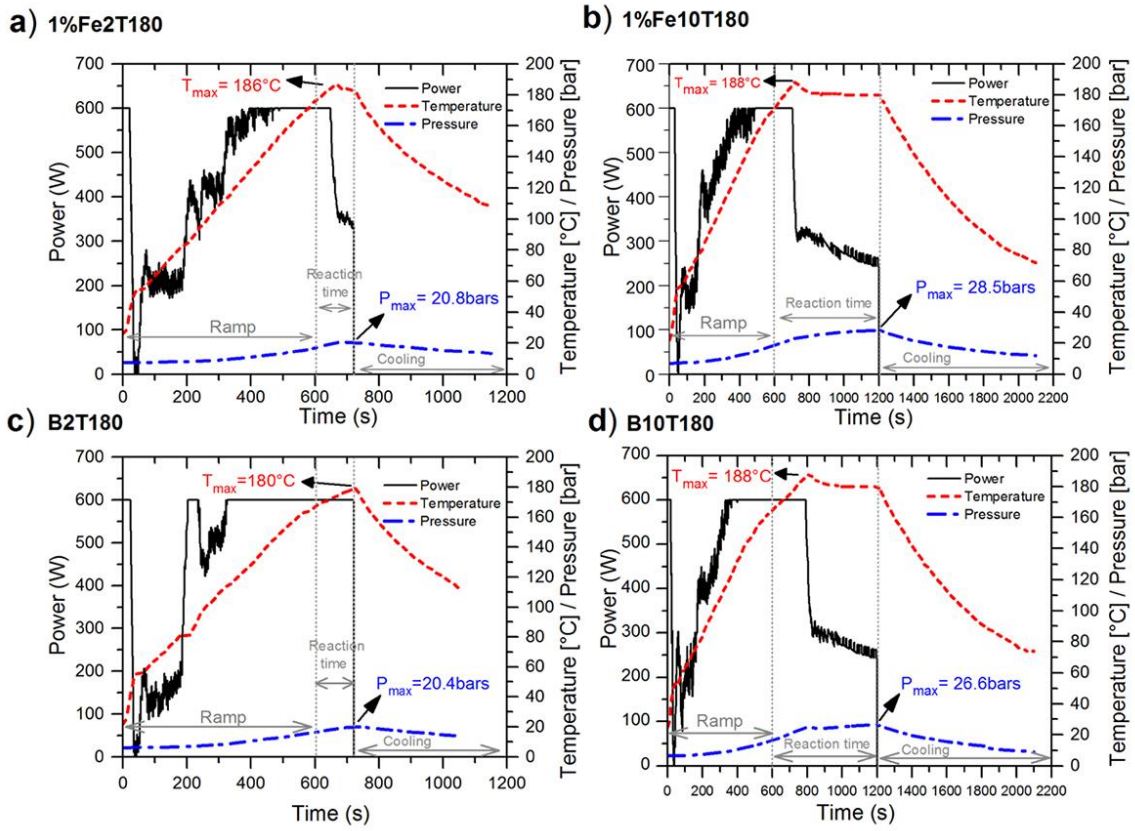

Figure 1. Conditions of temperature, pressure, and power within the microwave reactor; a) photocatalyst 1%Fe2T180, b) photocatalyst 1%Fe10T180, C) photocatalyst B2T180 and d) photocatalyst B10T180.

Source: Author's own elaboration.

It can be seen that the maximum pressure reached during the synthesis reactions for compounds at 2 min are less than the maximum pressure achieved by the compounds synthesized at 10 min, with a difference of 6.2 bar between compounds of TiO_2 without doping and 7.7 bars and the compounds of TiO_2 doped with 1% iron. This pressure increase occurred due to the exposure time of the microwaves with the polar reagent; the longer the time exposed to microwaves, the higher the vapor pressure generated and the higher the pressure in the system.

X-Ray Diffraction (XRD)

Figure 2 shows patterns of XRD of the synthesized compounds, 2 min and 10 min of reaction, *a*) and *b*), respectively. For each of the patterns analyzed, the presence of anatase crystalline phase of TiO_2 is observed, as the characteristic diffraction peaks of this phase according to the planes: (1 0 1), (0 0 4), (2 0 0), (1 0 5), (2 1 1), and (2 0 4) (Ogawa & Abe, 1981). It is also noted that the shape and intensity of the diffraction peaks of crystal planes for each compound are quite similar despite the difference in time of synthesis. However, in figure 2b, for compounds of higher percentage of iron, it is possible to note a slight broadening and reduced intensity for the peak of the anatase phase (204). This effect could be caused by a distortion in the crystal structure due to replacing the Ti^{4+} by ion Fe, resulting in specific crystallographic defects (Yalcın, Kılıc & Cınar, 2010). This small decrease in crystallinity can be due to the decrease in the growth kinetics of the anatase phase. It must be emphasized that, at 500 °C, heat treatment by other methods archive crystalline anatase phase or even the presence of rutile phase, so the synthesis method used caused a delay during the crystal growth process of the anatase phase.

ISSN online 2007-9621

An important aspect that must be noted is that no crystalline phase corresponding to Fe is observed even in the highest percentage employed (1% iron). One explanation is that these ions are dispersed in the anatase phase as a solid solution, since the presence of iron is confirmed by the results of EDS and UV-vis diffuse reflectance, as shown in the following sections. Another explanation is that the quantities of iron used are located below the limit visibility of X-rays analysis (Ravichandran, Selvam, Krishnakumar & Swaminathan, 2009).

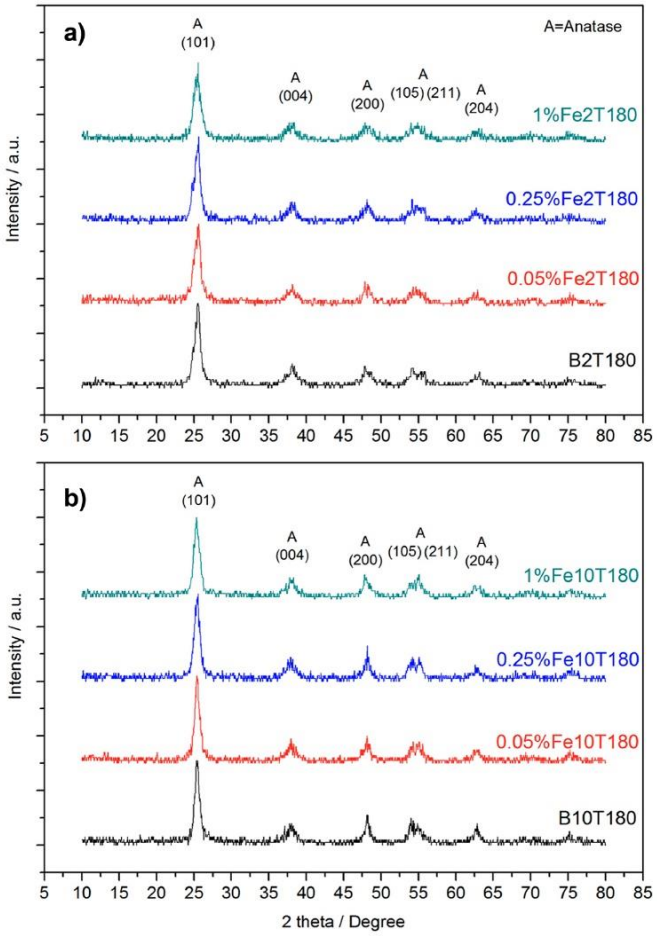

Figure 2. X-ray diffractograms of photocatalysts; *a*) 2 min of synthesis and *b*) 10 min of synthesis.

Source: Author's own elaboration.

Specific surface area (BET)

The values of BET of the synthesized photocatalysts are shown in table 2. It was observed that the introduction of iron caused an increase in the surface area. The doping of iron ions within the range of suitable concentration can lead to an increase in surface area because, with this doping, agglomeration of particles and form nanocrystalline powders with high surface can be prevented (Asiltür, Sayllkan & Arpaç, 2009; Song, Jun, Chen & Jianjun, 2011). It is noted that, in all compounds synthesized at 10 min reactions, there was a slight increase in BET as the amount of iron introduced is increased, taking a difference between the undoped compound and 1% iron doped compound of 12.5 m^2g^{-1}.

Table 2. Specific surface area of the synthesized photocatalysts.

ISSN online 2007-9621

Compound	Specific surface area (m^2/g)
B10T180	95.0
B2T180	105.7
0.05%Fe10T180	103.5
0.05%Fe2T180	110.3
0.25%Fe10T180	105.6
0.25%Fe2T180	113.3
1%Fe10T180	129.8
1%Fe2T180	117.2

Source: Author's own elaboration.

Scanning electron microscopy (SEM) and EDS

Figure 3 shows the micrographs at 100 000X of the materials in *a*) and *b*) undoped photocatalists B10T180 and B2T180, respectively, and in *c*) and *d*) of the photocatalists 1%Fe10T180 and 1%Fe2T180, respectively. The presence of nanoparticles in all cases can be seen. However, these ones are bonded to each other in irregular shapes with different sizes; in the case of the materials, doped smaller agglomerates are formed. Smaller agglomerates for 1% iron doped samples may have led to increased BET compared to the compounds of undoped TiO_2 (see section BET).

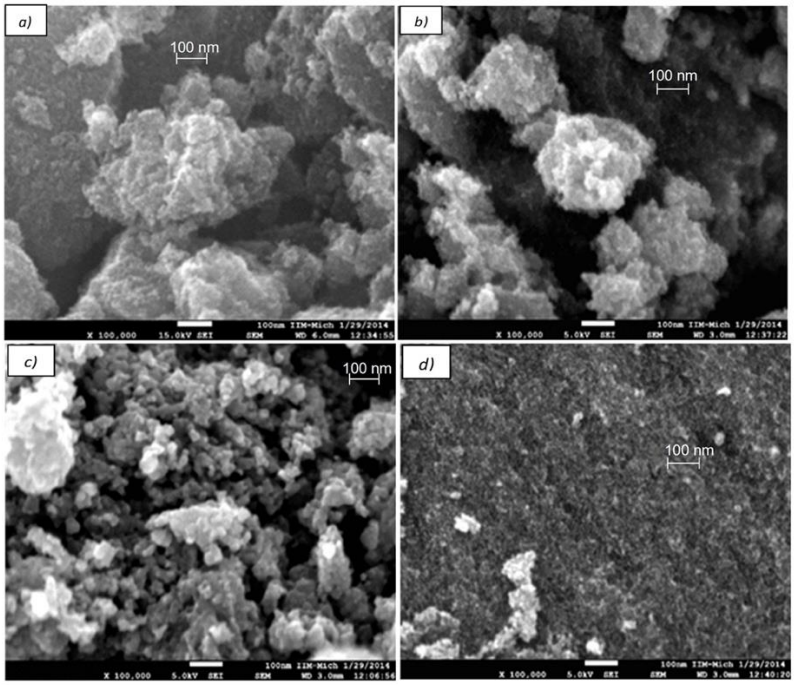

Figure 3. SEM micrographs to 100 000X resolution: *a*) photocatalyst B10T180, *b*) photocatalyst B2T180, *c*) photocatalyst 1%Fe10T180 and *d*) photocatalyst 1%Fe2T180.

Source: Author's own elaboration.

Figure 4 shows EDS images of the compounds B2T180 (subsection a), 1%Fe2T180 (subsection b), and 1%Fe10T180 (subsection c), where it is observed that peaks for compound B2T180 are about 0.4

ISSN online 2007-9621

keV, 4.5 keV to 5 keV, corresponding to the titanium atoms which are located in both the lattice and on the TiO_2 surface and a peak around 0.5 keV, which correspond to the oxygen atom of the crystal lattice of TiO_2. In the case of compound 1%Fe2T180 and 1% Fe10T180, as well as B2T180, the corresponding peak to titanium and oxygen are present. Additionally, these peaks are obtained at 6.4 keV and 0.75 keV, corresponding to the iron atoms which are observed located on the surface of TiO_2. These iron peaks are observed at a low proportion due to low amount of iron that was used for doping (1% iron); the latter results confirm the existence of Fe atoms for compounds doped 1% iron; however, patterns in XRD (figure 2) show no peaks related to Fe. Likewise, it is possible to observe images representative of peaks of copper, nickel, and carbon due to sample preparation, as this was fixed with a carbon-based resin and the sample holder used was made of an alloy taining copper and nickel.

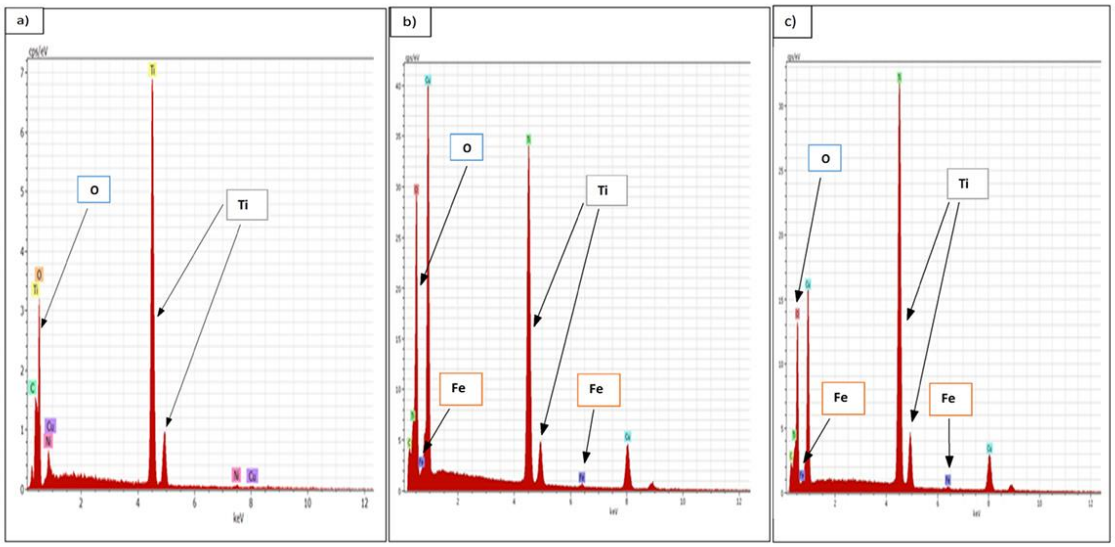

Figure 4. Images of EDS; *a*) photocatalyst B2T180, *b*) photocatalyst 1%Fe2T180 and *c*) photocatalyst 1%Fe10T180.

Source: Author's own elaboration.

UV-vis diffuse reflectance spectroscopy

Figure 5 shows diffuse reflectance spectra of synthesized compounds at 2 min and 10 min of reaction, *a*) and *b*), respectively, at the different percentages of iron (0%, 0.05%, 0.25%, and 1% iron). It is observed that these mostly absorb the ultraviolet region and decreasing the intensity of absorbance as it approaches to the visible region. For undoped compounds, B2T180 and B10T180 have a small intensity of absorbance in the visible spectrum at 400 nm wavelength, which decreases from 0 nm to 440 nm, about 0.05% iron doped compound (0.05%Fe2T180 and 0.05%Fe10T180). They have a small visible absorbance at 400 nm, which decreases from 0 nm to 460 nm range, with a slight shift to longer wavelengths (red shift). The 0.25% iron doped compound (0.25%Fe2T180 and 0.25%Fe10T180) and 1% iron (1%Fe2T180 and 1%Fe10T180) show an even greater shift of the visible absorption spectrum as these have a higher absorbance in the range from 400 nm to 600 nm wavelength. Pang & Abdullah (2012) disclose that these changes in the electronic structure are indeed due the introduction of Fe^{+3} TiO_2 network.

ISSN online 2007-9621

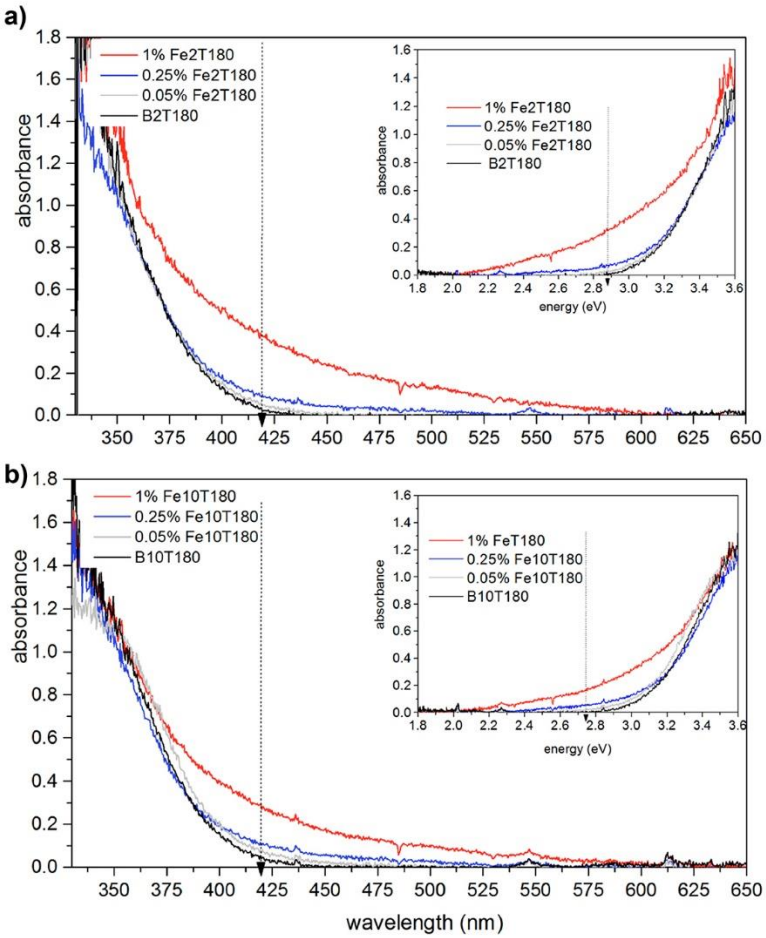

Figure 5. UV-vis diffuse reflectance of the synthesized photocatalysts; *a*) 2 min of synthesis and *b*) 10 min of synthesis. The direction of the vertical dotted line indicates only the order of the samples.

Source: Author's own elaboration.

Photocatalytic activity

Figure 6 shows the results of the discoloration of the AB9 dye by photocatalysts synthesized to 2 min and 10 min of reaction *a*) and *b*), respectively. These were compared with the photolysis lamp employed and the commercial photocatalyst Degussa P-25. It was observed that there was no discoloration of the colorant by photolysis, and the commercial photocatalyst Degussa P-25 degraded the 100% of the dye in 30 min of reactions. In the case of the synthesized photocatalysts, the ones that presented greater photocatalytic activity were the compounds without doping. The compound synthesized at 10 min (B10T180) degraded 100% of the dye in 60 min of reaction and the compound synthesized at 2 min (B2T180) degraded the 100% of the dye in 45 min of reaction. In general, a decrease is observed in photocatalytic activity as the amount of incorporated iron was increased. However, the compounds synthesized at 2 min reaction obtained greater photocatalytic activity than the synthesized 10 min reaction. This increase is attributed to the conditions generated during the synthesis, especially pressure. Samples synthesized at 10 min show higher pressure conditions due to longer exposure to microwaves (figure 1), which caused the decrease in the photocatalytic efficiency. However, it was not possible to visualize it through the characterization employed nor through the change

effect that caused the increase in pressure over the synthesized compounds. The negative effect of the discoloration of the AB9 dye by the addition of iron to TiO_2 may have occurred because the optimum doping was not found. This caused a decrease in generating radical •OH by the recombination pair electron-hole, which was provoked by the increase in absorption of visible spectrum (Zhang, Wang, Zakaria & Ying, 1998). Another reason may be that the microwave synthesis is not effective for preparing TiO_2-Fe photocatalyst, iron remains as Fe_2O_3 and it is not incorporated into the crystal lattice of TiO_2 (Esquivel *et al.*, 2013). A similar conclusion was obtained by Žabová & Církva (2009), where they said that the synthesis of TiO_2 photocatalysts doped with Fe^{+3} by microwave irradiation is not conducive for degradation of monochloroacetic acid and rhodamine B.

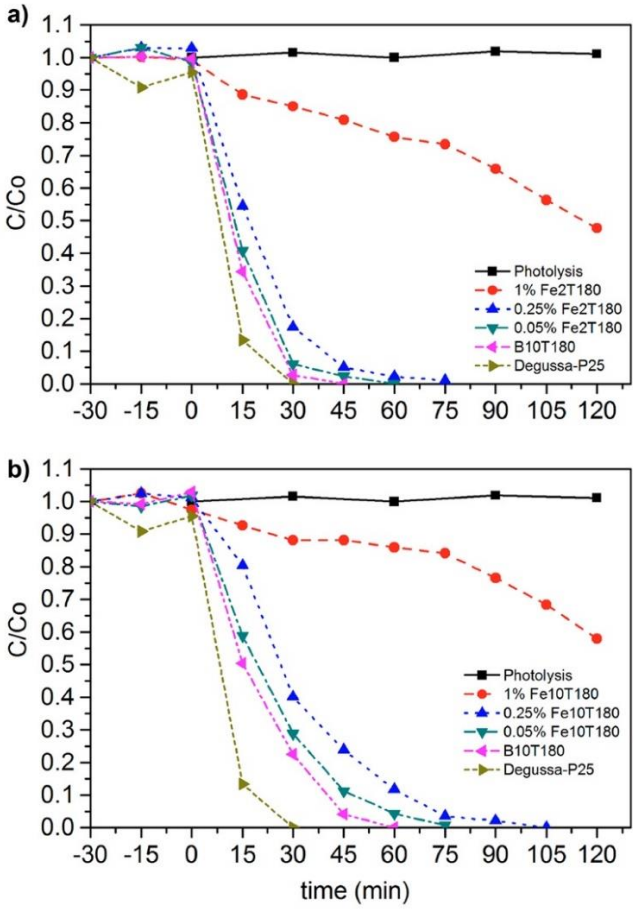

Figure 6. Graph of discoloration of the dye AB9 with synthesized photocatalysts; *a*) 2 min of synthesis and *b*) 10 min of synthesis.

Source: Author's own elaboration.

Conclusions

The synthesis of microwave assisted nanoparticles of TiO_2 and TiO_2-Fe was accomplished in approximately 35 min (excluding the drying and heat treatment), modifying their structural properties. It was observed that the microwave synthesis time at 180 °C indeed influences the photocatalytic activity of our synthesized photocatalysts, obtaining better results at 2 min than at 10 min; this is attributed to the conditions obtained during the synthesis, mainly the pressure. The undoped

compound B2T180 was the best photocatalyst synthesized, which obtained a 100% discoloration of AB9 dye at 45 min of irradiation with UV light, approaching to discoloration times of the commercial photocatalyst Degussa P-25. The results of BET of the synthesized compounds are in the order of 95 m^2g^{-1} to 130 m^2g^{-1} with an increase of BET under the increased percentage of iron in the compounds. It was also observed that the incorporation of iron to percentages from 0.05% to 1% decreases the photocatalytic activity of TiO_2 for the degradation of the AB9 dye.

Acknowledgments

Thanks to the support of CONACYT and the use of equipment, scientific and technical assistance of the Universidad Michoacana de San Nicolás de Hidalgo (UMNSH), Instituto Potosino de Investigación Científica y Tecnológica (IPICYT) and Universidad de Guanajuato (UG).

References

Abbas, K. (2009). Sol–gel synthesis, characterization, and catalytic activity of Fe(III) titanates. *Colloids and Surfaces A: Physicochemical and Engineering Aspects*, *346*(1-3), 130-137. doi: https://doi.org/10.1016/j.colsurfa.2009.06.003

Adán, C., Bahamonde, A., Fernández-García, M., & Martínez-Arias, A. (2007). Structure and activity of nanosized iron-doped anatase TiO_2 catalysts for phenol photocatalytic degradation. *Applied Catalysis B: Environmental, 72*(1-2), 11–17. doi: https://doi.org/10.1016/j.apcatb.2006.09.018

Alijani, H., & Shariatinia, Z. (2017). Effective aqueous arsenic removal using zero valent iron doped MWCNT synthesized by in situ CVD method using natural α-Fe_2O_3 as a precursor. *Chemosphere*, *171*, 502-511. doi: https://doi.org/10.1016/j.chemosphere.2016.12.106

Asiltür, M., Sayllkan, F., & Arpaç, E. (2009). Effect of Fe^{3+} ion doping to TiO_2 on the photocatalytic degradation of Malachite Green dye under UV and vis-irradiation Photochem. *Journal of Photochemistry and Photobiology A: Chemistry, 203*(1), 64–71. doi: https://doi.org/10.1016/j.jphotochem.2008.12.021

Choi, W., Termin, A., & Hoffmann, M. R. (1994). The role of metal ion dopants in quantum-sized TiO_2: correlation between photoreactivity and charge carrier recombination dynamics *Journal of Physical Chemistry*, *98*(51), 13669–13679. doi: https://doi.org/10.1021/j100102a038

Doong, R. A., Chang, P. Y., & Huang, C. H. (2009). Microstructural and photocatalytic properties of sol‑gel-derived vanadium-doped mesoporous titanium dioxide nanoparticles. *Journal of Non-Crystalline Solids*, *355*(45-47), 2302–2308. doi: https://doi.org/10.1016/j.jnoncrysol.2009.07.017

Esquivel, K., Nava, R., Zamudio-Méndez, A., Vega González, M., Jaime-Acuña, O. E., Escobar-Alarcón, L., Peralta-Hernández, J. M., Pawelec, B., & Fierro, J. L. G. (2013). Microwave-assisted synthesis of (S)Fe/TiO_2 systems: Effects of synthesis conditions and dopant concentration on photoactivity. *Applied Catalysis B: Environmental*, *140-141*, 213–224. doi: https://doi.org/10.1016/j.apcatb.2013.03.047

Gladfelter, W. L. (2011). Uncovering the transformations that occur during the early stages of TiO_2 CVD on Si (A perspective on the article, "TiO_2 chemical vapor deposition on Si(111) in ultrahigh vacuum: Transition from interfacial phase to crystalline phase in the reaction limited regime" by A. Sandell *et al.*). *Surface Science*, *605*(13-14), 1146. doi: https://doi.org/10.1016/j.susc.2011.04.027

Hamedani, N. F., Mahjoub, A. R., Khodadadi, A. A., & Mortazavi, Y. (2011). Microwave assisted fast synthesis of various ZnO morphologies for selective detection of CO, CH_4 and ethanol. *Sensors and Actuators B: Chemical*, *156*(2), 737–742. doi: https://doi.org/10.1016/j.snb.2011.02.028

Khade, G. V., Suwarnkar, M. B., Gavade, N. L., & Garadkar, K. M. (2015). Green synthesis of TiO_2 and its photocatalytic activity. *Journal of Materials Science: Materials in Electronics*, *26*(5), 3309–3315. doi: https://doi.org/10.1007/s10854-015-2832-7

Kim, D. H., Lee, K. S., Kim, Y. S., Chung, Y. C., & Kim, S. J. (2006). Photocatalytic Activity of Ni 8 wt%-doped TiO_2 photocatalyst synthesized by mechanical alloying under visible light. *Journal of the American Ceramic Society*, *89*(2), 515–518. doi: https://doi.org/10.1111/j.1551-2916.2005.00782.x

Komarneni, S., Rajha, R. K., & Katsuki, H. (1999). Microwave-hydrothermal processing of titanium dioxide. *Materials Chemistry and Physics*, *61*(1), 50-54. doi: https://doi.org/10.1016/S0254-0584(99)00113-3

López-Muñoz, M. J., Arencibia, A., Segura, J. M., & Raez, J. M. (2017). Removal of As(III) from aqueous solutions through simultaneous photocatalytic oxidation and adsorption by TiO_2 and zero-valent iron. *Catalysis Today*, *280*(1), 149-154. doi: https://doi.org/10.1016/j.cattod.2016.05.043

Mali, S. S., Shinde, P. S., Betty, C. A., Bhosale, P. N., Lee, W. J., & Patil, P. S. (2011). Nanocoral architecture of TiO_2 by hydrothermal process: Synthesis and characterization. *Applied Surface Science*, *257*(23), 9737-9746. doi: https://doi.org/10.1016/j.apsusc.2011.05.119

Ocakoglu, K., Mansour, Sh. A., Yildirimcan, S., Al-Ghamdi, A. A., El-Tantawy, F., & Yakuphanoglu, F. (2015). Microwave-assisted hydrothermal synthesis and characterization of ZnO Nanorods. *Spectrochimica Acta Part A: Molecular and Biomolecular Spectroscopy*, *148*, 362–368. doi: https://doi.org/10.1016/j.saa.2015.03.106

Ogawa, H., Abe, A., Nishikawa, M., & Hayakawa, S. (1981). Preparation of tin oxide films from ultrafine particles. *Journal of the Electrochemical Society*, *128*(3), 685-689. doi: https://doi.org/10.1002/chin.198129037

Pang, Y. L., & Abdullah, A. Z. (2012). Effect of low Fe^{3+} doping on characteristics, sonocatalytic activity and reusability of TiO_2 nanotubes catalysts for removal of Rhodamine B from water. *Journal of Hazardous Materials*, *2*35–236, 326–335. doi: https://doi.org/10.1016/j.jhazmat.2012.08.008

Perera, S., & Gillan, E. G. (2008). A facile solvothermal route to photocatalytically active nanocrystalline anatase TiO_2 from peroxide precursors. *Solid State Sciences*, *10*(7), 864-872. doi: https://doi.org/10.1016/j.solidstatesciences.2007.10.032

Ravichandran, L., Selvam, K., Krishnakumar, B., & Swaminathan, M. (2009). Photovalorisation of pentafluorobenzoic acid with platinum doped TiO_2. *Journal of Hazardous Materials*, *167*(1-3), 763–769. doi: https://doi.org/10.1016/j.jhazmat.2009.01.048

Shojaie, A. F., & Loghmani, M. H. (2010). La^{3+} and Zr^{4+} co-doped anatase nano TiO_2 by sol-microwave method. *Chemical Engineering Journal, 157*(1), 263–269. doi: https://doi.org/10.1016/j.cej.2009.12.025

Song, H., You, S., Chen, T., & Jia, X. (2015). Controlled preparation of TiO_2 hollow microspheres constructed by crosslinked nanochains with high photocatalytic activity. *Journal of Materials Science: Materials in Electronics, 26*(11), 8442–8450. doi: https://doi.org/10.1007/s10854-015-3513-2

Song, S., Jun, B., Chen, G., & Jianjun, D. (2011). Photocatalytic degradation of gaseous o-xylene over M-TiO_2 (M=Ag, Fe, Cu, Co) in different humidity levels under visible-light irradiation: activity and kinetic study. *Rare Metals*, *30*(1), 147–152. doi: https://doi.org/10.1007/s12598-011-0258-9

Suzuki, A., Yamaguchi, H., Kageyama, H., Oaki, Y., & Imai, H. (2015). Microwave-assisted rapid synthesis of anatase TiO_2 nanosized particles in an ionic liquid-water system. *Journal of the Ceramic Society of Japan*, *123*, 79-82. doi: https://doi.org/10.2109/jcersj2.123.79

Tian, F., Wu, Z., Chen, Q., Yan, Y., Cravotto, G., & Wu, Z. (2015). Microwave-induced crystallization of AC/TiO_2 for improving the performance of rhodamine B dye degradation. *Applied Surface Science*, *351*(1), 104–112. doi: https://doi.org/10.1016/j.apsusc.2015.05.133

Wang, M. C., Lin, H. J., & Yang, T. S. (2009). Characteristics and optical properties of iron ion (Fe^{3+})-doped titanium oxide thin films prepared by a sol–gel spin coating. *Journal of Alloys and Compounds*, *473*(1-2), 394–400.doi: https://doi.org/10.1016/j.jallcom.2008.05.105

Xiang Y., Wang X., Zhang X., Hou H., Dai K., Huang Q., & Chen H. (2018). Enhanced visible light photocatalytic activity of TiO_2 assisted by organic semiconductors: a structure optimization strategy of conjugated polymers. *Journal of Material Chemistry A*, *6*(1), 153-159. doi: https://doi.org/10.1039/c7ta09374h

Yalçın, Y., Kılıç, M., & Çınar, Z. (2010). Fe^{+3}-doped TiO_2: A combined experimental and computational approach to the evaluation of visible light activity. *Applied Catalysis B: Environmental*, *99*(3-4), 469–477. doi: https://doi.org/10.1016/j.apcatb.2010.05.013

Yan, L., Tu H., Chan T., & Jing C. (2017). Mechanistic study of simultaneous arsenic and fluoride removal using granular TiO_2-La adsorbent. *Chemical Engineering Journal, 313*, 983-992. doi: https://doi.org/10.1016/j.cej.2016.10.142

Yu, K. P., & Lee G. W. M. (2007). Decomposition of gas-phase toluene by the combination of ozone and photocatalytic oxidation process (TiO_2/UV, TiO_2/UV/O_3, and UV/O_3). *Applied Catalysis B: Environmental, 75*(1-29), 29–38. doi:https://doi.org/10.1016/j.apcatb.2007.03.006

Yu, X., & Shen, Z. (2011). Photocatalytic TiO_2 films deposited on cenosphere particles by pulse magnetron sputtering method. *Vacuum*, *85*(11), 1026-1031. doi: https://doi.org/10.1016/j.vacuum.2011.03.010

Žabová, H., & Církva, V. (2009). Microwave photocatalysis III. Transition metal ion-doped TiO_2 thin films on mercury electrodeless discharge lamps: preparation, characterization and their effect on the photocatalytic degradation of mono-chloroacetic acid and Rhodamine B. *Journal of Chemical Technology and Biotechnology*, *84*(11), 1624–1630. doi: https://doi.org/10.1002/jctb.2220

Zhang, Z., Wang, C. C., Zakaria, R., & Ying, J. Y. (1998). Role of particle size in Nanocrystalline TiO_2-based photocatalysts. *Journal of Physical Chemistry B*, *102*(52), 10871-10878. doi: https://doi.org/10.1021/jp982948+